

Ubiquitous rotating network magnetic fields and EUV cyclones in the quiet Sun

Jun Zhang¹ and Yang Liu²

ABSTRACT

We present the *Solar Dynamics Observatory* (SDO) Atmospheric Imaging Assembly (AIA) observations of EUV cyclones in the quiet Sun. These cyclones are rooted in the Rotating Network magnetic Fields (RNFs). Such cyclones can last several to more than ten hours, and, at the later phase, they are found to be associated with EUV brightenings (microflares) and even EUV waves. SDO Helioseismic and Magnetic Imager (HMI) observations show an ubiquitous presence of the RNFs. Using HMI line-of-sight magnetograms on 2010 July 8, we find 388 RNFs in an area of 800×980 square arcseconds near the disk center where no active region is present. The sense of rotation shows a weak hemisphere preference. The unsigned magnetic flux of the RNFs is about 4.0×10^{21} Mx, or 78% of the total network flux. These observational phenomena at small scale reported in this letter are consistent with those at large scale in active regions. The ubiquitous RNFs and EUV cyclones over the quiet Sun may suggest an effective way to heat the corona.

Subject headings: Sun: corona —Sun: UV radiation —Sun: magnetic fields

1. INTRODUCTION

In the past 20 years, observations from space-based telescopes revealed that the solar corona and transition region are much more dynamic than had been thought. Surges, jets, macrospicules, bright points and macroflares take place everywhere in the solar atmosphere. Sometimes, surges, jets and macrospicules exhibit rotating motions (Pike & Mason 1998; Zhang et al. 2000a; Patsourakos et al. 2008; Liu et al. 2009; Kamio et al. 2010), which is

¹Key Laboratory of Solar Activity, National Astronomical Observatories, Chinese Academy of Sciences, Beijing 100012, China; E-mail: zjun@nao.cas.cn

²W. W. Hansen Experimental Physical Laboratory, Stanford University, Stanford, CA 94305, USA; E-mail: yliu@sun.stanford.edu

suggested to be an indicator of the existence of Alfvén waves in these structures (Sterling, 1998). The mechanism providing such a highly dynamic corona and transition region is considered to be related to the long-standing puzzle of how the corona is heated to a million Kelvin (Aschwanden 2004).

Rotational motions in the photosphere (Brandt et al 1988) may create rotating motions of surges (jets) and macrospicules which are driven by localized downdrafts that collect the cold plasma returning to the solar interior after releasing internal energy (e.g., Spruit et al. 1990; Stein & Nordlund 1998). Usually those vortices are small (0.5 Mm) and last several minutes, but sometimes they could be large and survive much longer (see, e.g. Attie et al. 2009). In the quiet Sun, about 3.1×10^{-3} vortices $\text{Mm}^{-2} \text{ minute}^{-1}$ are found (Bonet et al. 2010), and they do not have a preferred rotation sense on the different hemispheres (Bonet et al. 2008). The vortices on the photosphere can propagate upward along the field lines (e.g., Choudhuri et al. 1993; Zirker 1993; van Ballegooijen et al. 1998), and govern the evolution of magnetic footpoints (Balmaceda et al. 2010). In the low chromosphere, vortical motions with possible propagation of waves were also detected for the first time by Wedemeyer-Böhm & Rouppe van der Voort (2009). Moreover, they often wind up opposite polarity field lines, facilitating magnetic reconnection and ensuing energy release. For active regions, rotating motion is one of the most important processes for sunspot evolution, and may be responsible for the flaring (Gerrard et al. 2003). Thus those rotating motions may provide a mechanism to build up the magnetic energy in the corona that is eventually released during transients, which in turn heats the corona.

In this Letter, we report the discovery of EUV cyclones and Rotating Network magnetic Fields (RNFs) in the quiet Sun with the observations from the Atmospheric Imaging Assembly (AIA; Lemen et al. 2011) and the Helioseismic and Magnetic Imager (HMI; Wachter et al. 2011) aboard the *Solar Dynamics Observatory* (SDO). The paper is organized as follow. In Section 2 we describe the observational data we use. An analysis of the data is presented in Section 3. In Section 4, we conclude this study and discuss the results.

2. OBSERVATIONS

SDO/AIA observes uninterruptedly the Sun’s full disk at 10 wavelengths at a 12-second cadence and a $0.6'' \text{ pixel}^{-1}$ sampling. The measurements reflect various temperatures of the solar atmosphere (from $\sim 5000 \text{ K}$ to $\sim 2.5 \text{ MK}$) from the photosphere to the corona. SDO/HMI, from polarization measurements, information such as Doppler-velocity, line-of-sight (LOS) magnetic field strength, and vectorial information of the magnetic field are obtained. The data cover the full disk of the Sun with a spatial sampling of $0.5'' \text{ pixel}^{-1}$.

The full disk LOS magnetograms, used in this Letter, are taken at a cadence of 45 seconds.

3. ANALYSIS

The phenomenon of the EUV cyclones is seen everywhere in the quiet Sun in the AIA data in all EUV channels of 171, 193, 304, 211, 131, 335, and 94 Å. Those cyclones are found to be associated with the magnetic fields that show conspicuous rotation when viewed with the movies of the HMI time-series magnetograms. We use the term RNFs to refer to those rotating magnetic fields. Here we present two examples of the EUV cyclones to demonstrate their evolutionary characteristics and properties. Shown in Figures. 1(A) and 1(B) is a cyclone occurred on July 2 (see also movie1). The images were taken in the 171 Å channel. This cyclone was in the northern hemisphere, close to the solar equator. It started at $\sim 2:00$ UT, rotated counter-clockwisely, and lasted 12 hours. The footpoint of the cyclone on the photosphere, shown as a positive field patch in the HMI LOS magnetograms (the white feature in Figures. 1(C) and 1(D)), also rotated counter-clockwisely. At 04:02:48 UT, the magnetic flux in this patch was 2.9×10^{19} Mx, one order greater than the flux in a typical network element ($\sim 10^{18}$ Mx, Zhang et al. 2006). The noise level of HMI 45 s magnetograms is 10.2 Mx cm^{-2} (Liu et al. 2011), and the minimum flux obtained for this level in HMI is 1.3×10^{16} Mx. Its longer axis was along the northeast-southwest direction. At 06:44:48 UT, this axis rotated to southeast-northwest direction. It suggests that the magnetic field rotated 64° within 162 minutes.

The other example was in the southern hemisphere on July 20. It occurred at 07:00 UT, and lasted 9 hours. Figures. 2 (A) and (B) show the cyclone at the 171 Å images. The two circles denote the place where a time-slice map is made. Different from the cyclone on July 2, this cyclone rotated clockwisely (see movie2). From 11:23:48 UT to 13:20:48 UT, the positive magnetic fields (black contours in Figures 2(C) and 2(D)), which the cyclone are rooted in, rotated 83° clockwisely (see (C) and (D) in Figure 2) with a speed of $0.8^\circ \text{ min}^{-1}$. Its flux is about 1.6×10^{19} Mx and then it cancelled with the nearby negative elements (white contours in Figures 2(C) and 2(D)). We find that the negative polarity with an absolute magnetic flux of 3.6×10^{18} Mx disappeared and the positive polarity faded about 3.9×10^{18} Mx during the cancellation. The blue curve in panel (D) is the contour of EUV brightening in panel (B). We can see that the brightening corresponds to the neutral region, instead to the positive polarity. Figure 2 (E) shows a time-slice map of the AIA 171 Å images. The X-axis refers to time, running from 2010 July 20 11:00 UT to 15:00 UT. The Y-axis refers to the angle subtended by the dotted curves measured clockwisely, whose origin is the center of the circle and the reference direction is the West, as shown in Panel (A). The dashed curve outlines

the intersection of the leading boundary of the cyclone. In the 3-hour time interval (from 11:00 UT to 14:00 UT), the cyclone rotated about 360° . In the later phase of the cyclone at 14:26:59 UT, an EUV brightening appeared. This brightening continuously developed, exhibiting subtle structures, and becoming a two-ribbon microflare (the white patches in Figure 3). It lasted 2 hours, and disappeared at 16:18:11 UT. Meanwhile a small-scale wave was triggered by the microflare. It propagated with an average speed of 45 km s^{-1} , and lasted almost 8 minutes. Its disturbance spread over an area of $6.3 \times 10^8 \text{ km}^2$, equivalent to a typical supergranular cell.

Figure 4(A) shows the angular speed of the cyclone measured from the time-slice map. It indicates that the cyclone underwent two acceleration processes. At first the cyclone rotated with an angular speed of 1° min^{-1} , 50 minutes later the speed reached 7° min^{-1} , and then slowed down to 1° min^{-1} again. At 13:20 UT, the cyclone accelerated again. The speed reached another peak ($4.8^\circ \text{ min}^{-1}$). Figure 4(B) shows the propagating speed of the EUV wave. We determine the wave front (denoted by stars in each panel in Figure 3) every 36-second, and then compute the mean speed in the 36-second period. The propagation speed of the wave was not constant. There were two peaks, ($\sim 80 \text{ km s}^{-1}$ at 16:00:06 UT, and 85 km s^{-1} at 16:05:30 UT).

Observations have shown that EUV cyclones are rooted in the RNFs. An interesting question is then: how many RNFs are there on the solar surface? To answer this question, we surveyed the 2010 July 8 AIA/HMI data when no active region was present on the solar disk. In an area of 800×980 square arcseconds near the disk center, we found 388 RNFs (movie3 shows an example of the RNFs). The occurrence of these events is $4.9 \times 10^{-4} \text{ arcsec}^{-2} \text{ day}^{-1}$. The average lifetime of the RNFs is about 3.5 h. The distribution of these RNFs is plotted in Figure 5. Their magnetic fluxes range from $1.24 \times 10^{17} \text{ Mx}$ to $5.85 \times 10^{19} \text{ Mx}$. The average flux is $1.03 \times 10^{19} \text{ Mx}$, and the total flux of these RNFs is about $4.0 \times 10^{21} \text{ Mx}$, or 78% of the unsigned magnetic flux in that area. There are 179 and 209 RNFs in the northern and southern hemispheres, respectively. The sense of the rotation shows a weak hemisphere preference: 61% of the RNFs in the northern hemisphere (109 of the 179 RNFs) rotated counter-clockwisely, while 56% of the RNFs in the northern hemisphere (116 of 209 RNFs) rotated clockwisely. It leads to 5600 RNFs over the entire solar surface each day. It infers that a total flux of $5.8 \times 10^{22} \text{ Mx}$ is rotating. Simultaneous AIA observations show that among the cyclones relevant to these RNFs, 231 ones ($\sim 60\%$ of the total) are associated with microflares.

4. DISCUSSION AND CONCLUSIONS

In this Letter we report the discovery of EUV cyclones in the quiet Sun. They are rooted in the RNFs, and last several to more than ten hours, evidently different from surges (jets) and macrospicules, which have lifetimes less than one hour (Zhang et al. 2000b). About 60% EUV cyclones are associated with microflares and even small-scale EUV waves at the later phase of cyclones. The microflares correspond to the neutral region, instead to one polarity. HMI observations show the ubiquitous presence of the RNFs. The sense of rotation shows a weak hemisphere preference, which is also presented with G-band observations in Vargas Domínguez et al. (2011). The average magnetic flux is 1.03×10^{19} Mx. Every day, we infer that about 5600 RNFs are present over the entire solar surface. The total unsigned flux is about 5.8×10^{22} Mx.

As revealed in this study, the brightenings (microflares) are not corresponding to one polarity but to the neutral place where the opposite polarities cancelled. This is consistent with the morphological model shown in Figure 8 of Zhang et al. (2000b)., i.e, when two network elements with opposite polarities converge together and begin to cancel each other, a microflare appears at the cancelling site.

Surface motion on the photosphere is one of the two mechanisms proposed to build up the free energy in the corona (the other is the emergence of magnetic field). It can produce current sheets parallel to a separatrix that detach the interacting magnetic flux regions (Sweet 1969; Lau 1993; see Somov 2006 for a review). In the simulation of Gerrard et al. (2003), rotation of a sunspot with inflow of a pore leads to a strong build-up of current which is needed for magnetic reconnection. This current buildup is quite similar to the conclusion of Zhang et al. (2007, 2008), i.e., the rotational motions of sunspots relate to the transport of magnetic energy and complexity from the low atmosphere to the corona and play a key role in the onset of flares. In the quiet Sun, the random walk of the footpoints of coronal loops in the solar granulation is expected to cause the braiding of the field, which in turn leads to a multitude of coronal reconnection events (Schrijver 2007). Magnetic reconnection between sheared magnetic loops, indicating the injection of magnetic helicity of mixed signs, works as a trigger mechanism of solar flares (Kusano et al. 2004; Kusano 2005). Thus, the phenomena of RNFs, as well as the EUV cyclones, reported in this Letter, likely contain the process of energy buildup and release in solar corona.

What heats the solar corona remains one of the most important questions in solar physics and astrophysics. Klimchuk (2006) has proposed that three parts are involved to solve the coronal heating puzzle, which are (1) identifying a source of energy and a mechanism for converting the magnetic energy into heat, (2) determining how the plasma responds to the heating, and (3) predicting the spectrum of emitted radiation and its manifestation

as observable quantities. Our results may provide evidence to address the first two parts. Continuous development of RNFs braids field lines of the magnetic elements, manifested by the cyclones seen in the EUV observation. Magnetic reconnection then takes place in the braiding fields, releasing the stored energy that heats the corona. It is supported by the observed brightenings (microflares) and EUV waves.

Up to now, one of the most common mechanisms to heat the corona is the impulsive energy release (nanoflares, with times of minutes, and dimensions of Mms) that occurs in the small-scale magnetic fields (Parker 1988). AIA data indicate that microflares (or nanoflares) are not impulsive events. Furthermore, they are accompanied with other activities. For example, in the 2010 July 20 cyclone, the microflare occurred 7 hours after the cyclone, followed by a small-scale EUV wave. Small-scale waves in the quiet Sun may play a role in coronal heating: they transport energy to other places.

The small-scale EUV waves reported here propagate at a speed of 35–85 km s⁻¹, much slower than the EUV waves originate from active regions, which is in range of 200-400 km s⁻¹ (see, e.g., Thompson & Myers 2009). The nature of the small-scale waves is an interesting question that needs further investigation. It may provide additional information that helps understand the EUV waves that is still under intense debate (Wills-Davey & Thompson 1999; Wu et al. 2001; Ofman & Thompson 2002; Schmidt & Ofman 2010; Delannée 2000; Attrill et al. 2007; Attrill 2010; Liu et al. 2010).

The authors are indebted to the *SDO* teams for providing the data. This work is supported by the National Natural Science Foundations of China(G11025315, 40890161 and 10921303), the CAS Project KJCX2-YW-T04, and the National Basic Research Program of China under grant G2011CB811403.

REFERENCES

- Aschwanden, M. 2004, *Physics of the Solar Corona. An Introduction* (Springer-Verlag, Berlin)
- Attrill, G. D. R. 2010, *ApJ*, 718, 494
- Attrill, G. D. R., Harra, L. K., van Driel-Gesztelyi, L., & Démoulin, P. 2007, *ApJ*, 656, L101
- Attie, R., Innes, D. E., & Potts, H. E. 2009, *A&A*, 493, L13
- Balmaceda, L., Vargas Domínguez, S., Palacios, J., Cabello, I., & Domingo, V. 2010, *A&A*, 513, L6

- Bonet, J. A., Márquez, I., Sánchez Almeida, J., Cabello, I., & Domingo, V. 2008, *ApJ*, 687, L131
- Bonet, J. A. et al. 2010, *ApJ*, 723, L139
- Brandt, P. N., Scharmer, G. B., Ferguson, S., Shine, R. A., & Tarbell, T. D. 1988, *Nature*, 335, 238
- Choudhuri, A. R., Auffret, H., & Priest, E. R. 1993, *Sol. Phys.*, 143, 49
- Delannée, C. 2000, *ApJ*, 545, 512
- Gerrard, C. L., Brown, D. S., Mellor, D., Arber, T. D., & Hood, A. W. 2003, *Sol. Phys.*, 213, 39
- Kamio, S., Curdt, W., Teriaca, L., Inhester, B., & Solanki, S. K. 2010, *A&A*, 510, L1
- Klimchuk, J. A. 2006, *Sol. Phys.*, 234, 41
- Kusano, K., Maeshiro, T., Yokoyama, T., & Sakurai, T. 2004, *ApJ*, 610, 537
- Kusano, K. 2005, *ApJ*, 631, 1260
- Lau, Y. T. 1993, *Sol. Phys.*, 148, 301
- Lemen, J. R., Title, A. M., Akin, D. J., et al. 2011, *Sol. Phys.*, doi:10.1007/s11207-011-9776-8
- Liu, W., Berger, T. E., Title, A. M., & Tarbell, T. D. 2009, *ApJ*, 707, L37
- Liu, W., Nitta, N. V., Schrijver, C. J., Title, A. M., & Tarbell, T. D. 2010, *ApJ*, 723, L53
- Liu, Y., et al. 2011, *Sol. Phys.*, submitted
- Ofman, L., & Thompson, B. J. 2002, *ApJ*, 574, 440
- Parker, E. N. 1988, *ApJ*, 330, 474
- Patsourakos, S., Pariat, E., Vourlidas, A., Antiochos, S. K., & Wuelser, J. P. 2008, *ApJ*, 680, L73
- Pike, C. D., & Mason, H. E. 1998, *Sol. Phys.*, 182, 333
- Schrijver, C. J. 2007, *ApJ*, 662, L119
- Schmidt, J. M., & Ofman, L. 2010, *ApJ*, 713, 1008

- Somov, B. V. 2006, in *Plasma Astrophysics, Part I: Fundamentals and Practice* (New York: Springer)
- Spruit, H. C., Nordlund, A., & Title, A. M. 1990, *ARA&A*, 28, 263
- Stein, R. F., & Nordlund, A. 1998, *ApJ*, 499, 914
- Sterling, A. C. 1998, *ApJ*, 508, 916
- Sweet, P. A. 1969, *ARA&A*, 7, 149
- Thompson, B. J., & Myers, D. C. 2009, *ApJS*, 183, 225
- van Ballegooijen, A. A., Nisenson, P., Noyes, R. W., Lófdahl, M. G., Stein, R. F., Nordlund, Å., & Krishnakumar, V. 1998, *ApJ*, 509, 435
- Vargas Domínguez, S., Palacios, J., Balmaceda, L., Cabello, I., & Domingo, V. 2011, *MNRAS*, 416, 148
- Wachter, R., Schou, J., Rabello-Soares, M. C., et al. 2011, *Sol. Phys.*, doi:10.1007/s11207-011-9709-6
- Wedemeyer-Böhm, S., & Rouppe van der Voort, L. 2009, *A&A*, 507, L9
- Wills-Davey, M. J., & Thompson, B. J. 1999, *Sol. Phys.*, 190, 467
- Wu, S. T., Zheng, H., Wang, S., Thompson, B. J., Plunkett, S. P., Zhao, X. P., & Dryer, M. 2001, *J. Geophys. Res.*, 106, 25089
- Zhang, J., Li, L., & Song, Q. 2007, *ApJ*, 662, L35
- Zhang, J., Wang, J., & Liu, Y. 2000a, *A&A*, 361, 759
- Zhang, J., Wang, J., Lee, C., & Wang, H. 2000b, *Sol. Phys.*, 194, 59
- Zhang, J., Ma, J., & Wang, H. 2006, *ApJ*, 649, 464
- Zhang, Y., Liu, J., & Zhang, H. 2008, *Sol. Phys.*, 247, 39
- Zirker, J. B. 1993, *Sol. Phys.*, 147, 47

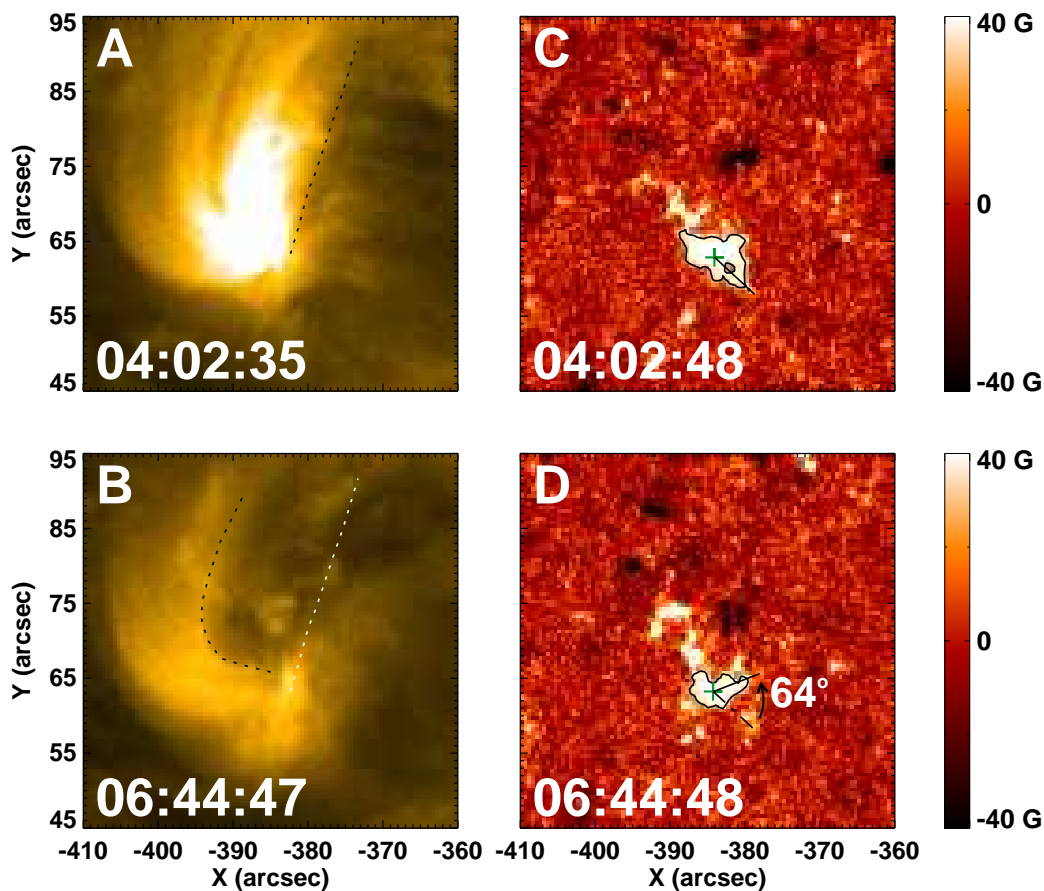


Fig. 1.— (A) and (B): Two AIA 171 Å images showing a cyclone on July 2, 2010 (see the accompanying movie1). The two black dashed curves outline one of the cyclone boundary at the two given times, and the white dashed curve in (B) is a duplicate of the black curve in (A). (C) and (D): Two corresponding HMI LOS magnetograms. The lines on the magnetograms denote the longer axis directions of the white patch which represents a positive RNF rooted in by the cyclone. In panels (C) and (D), the green plus symbols indicate the magnetic centroids, and the black curves are the contours of the positive magnetic elements at a level of 50 G. From 04:02:48 UT to 06:44:48 UT, the RNF rotated counter-clockwise 64°. For all images the North is upwards.

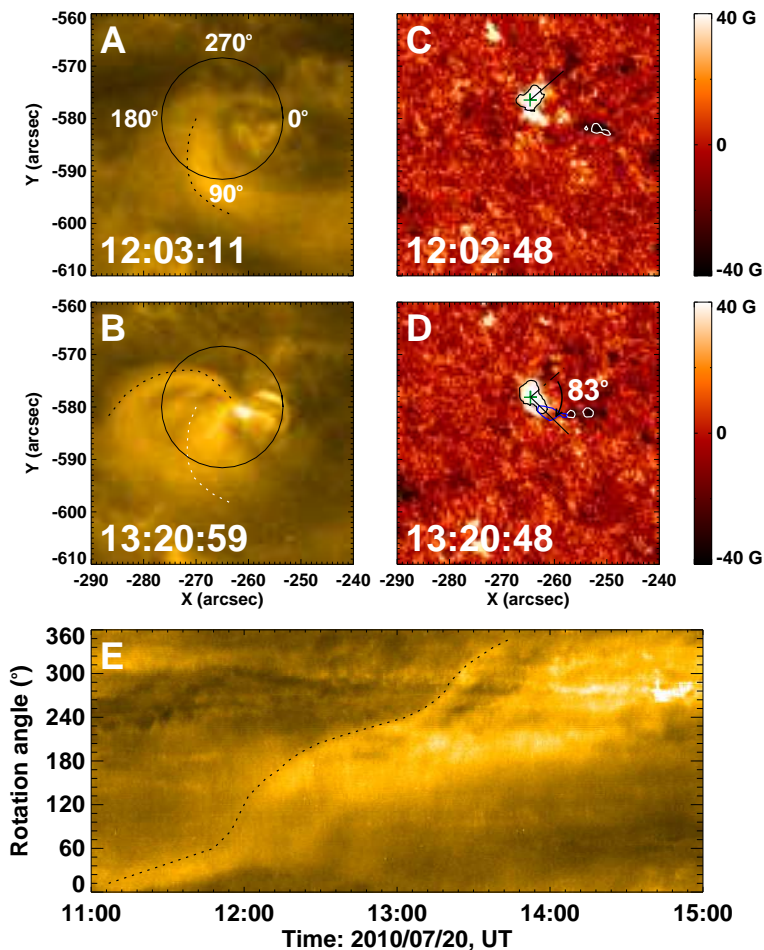


Fig. 2.— (A) and (B): Two AIA 171 Å images showing a cyclone on July 20, 2010 (see the accompanying movie²). The two circles represent the position at which a time-slice map is made, and the curves represent the boundary same as that in Figures. 1(A) and 1(B). (C) and (D): Two corresponding HMI magnetograms. The lines represent the directions similar to those in Figures. 1(C) and 1(D). In panels (C) and (D), the green plus symbols indicate the magnetic centroids, and the black and white curves are the contours of the positive (50 G) and negative (-50 G) magnetic elements, respectively. The blue curve in panel (D) is the contour of EUV brightening in panel (B). From 12:02:48 UT to 13:20:48 UT, the RNF rotated clockwise 83°. (E): A time-slice map taken from the AIA 171 Å images. The X-axis represents the time, running from 2010 July 20, 11:00 UT to 15:00 UT. The Y-axis denotes the angle at the center of the circle shown in panel (A), subtended by the arcs starting at the west (right) and measured in the clockwise direction. The dashed curve outlines the intersection of the leading boundary of the cyclone.

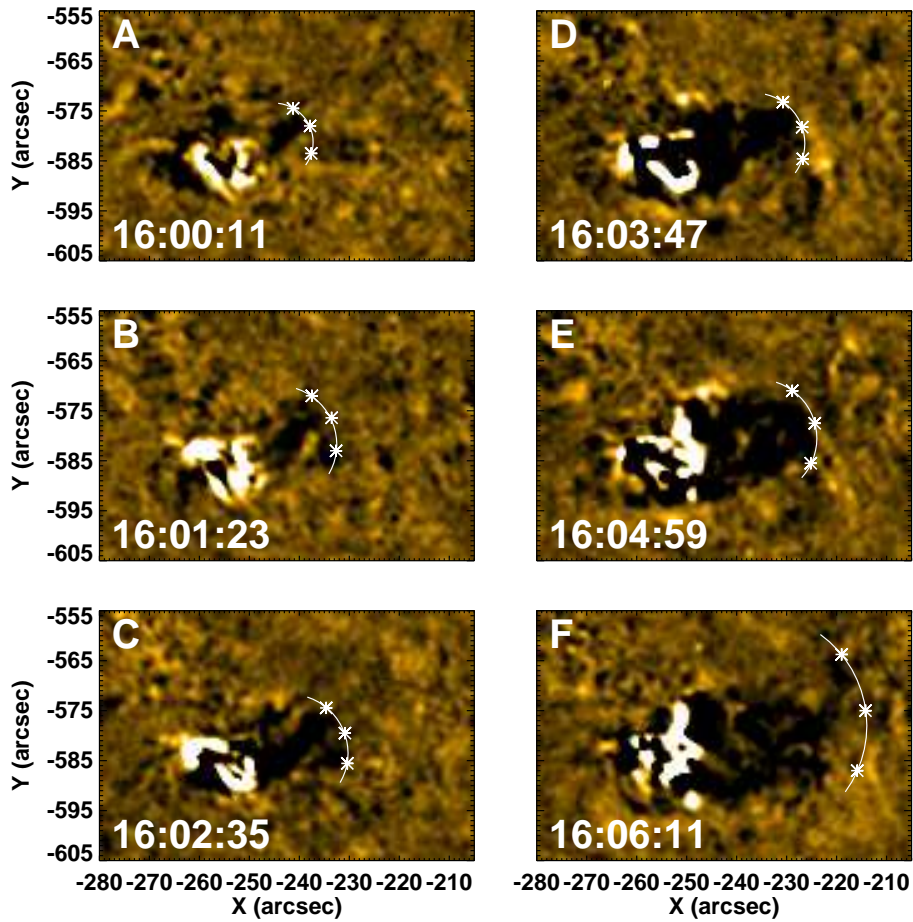


Fig. 3.— The time sequence of AIA 171 Å running difference images showing a microflare (white patches) and an EUV wave which follows the cyclone on July 20, 2010. Three stars on each map denote the locations of the wave front, and the propagating speed of this wave (Figure 4(B)) is determined from these locations.

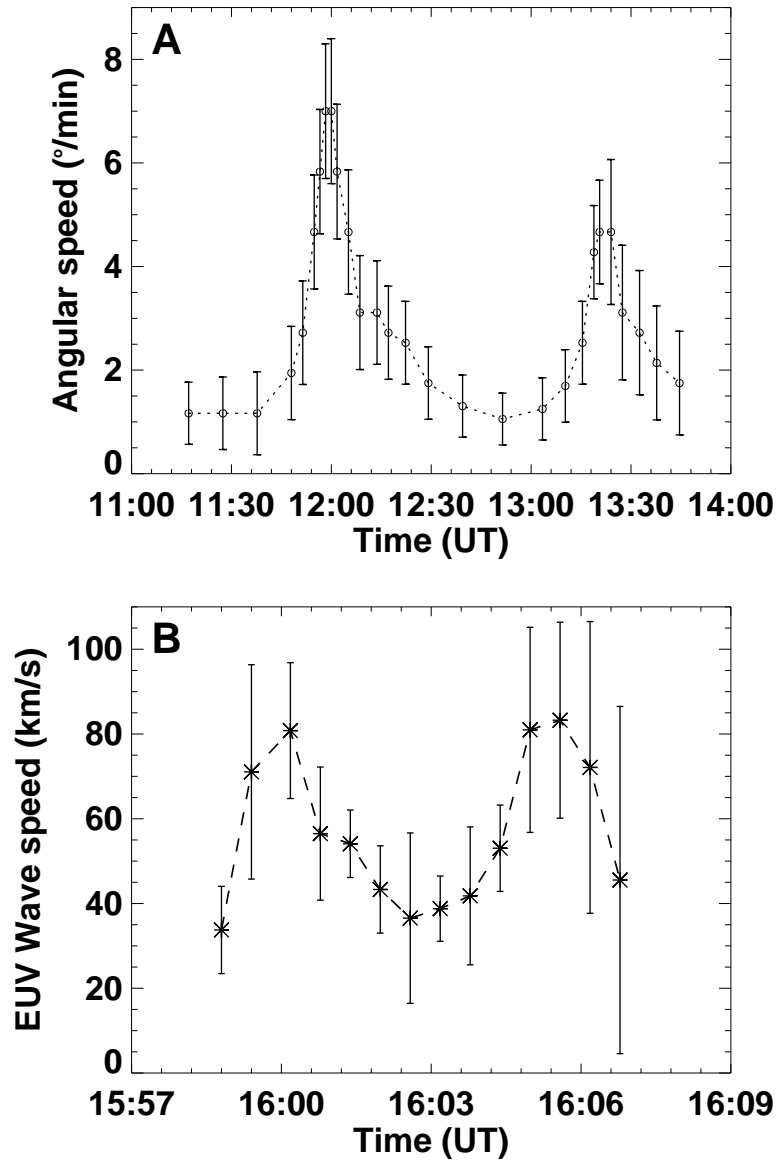


Fig. 4.— (A): Angular speed of the cyclone on July 20, 2010. (B): The propagating speed of the EUV wave displayed in Figure 3.

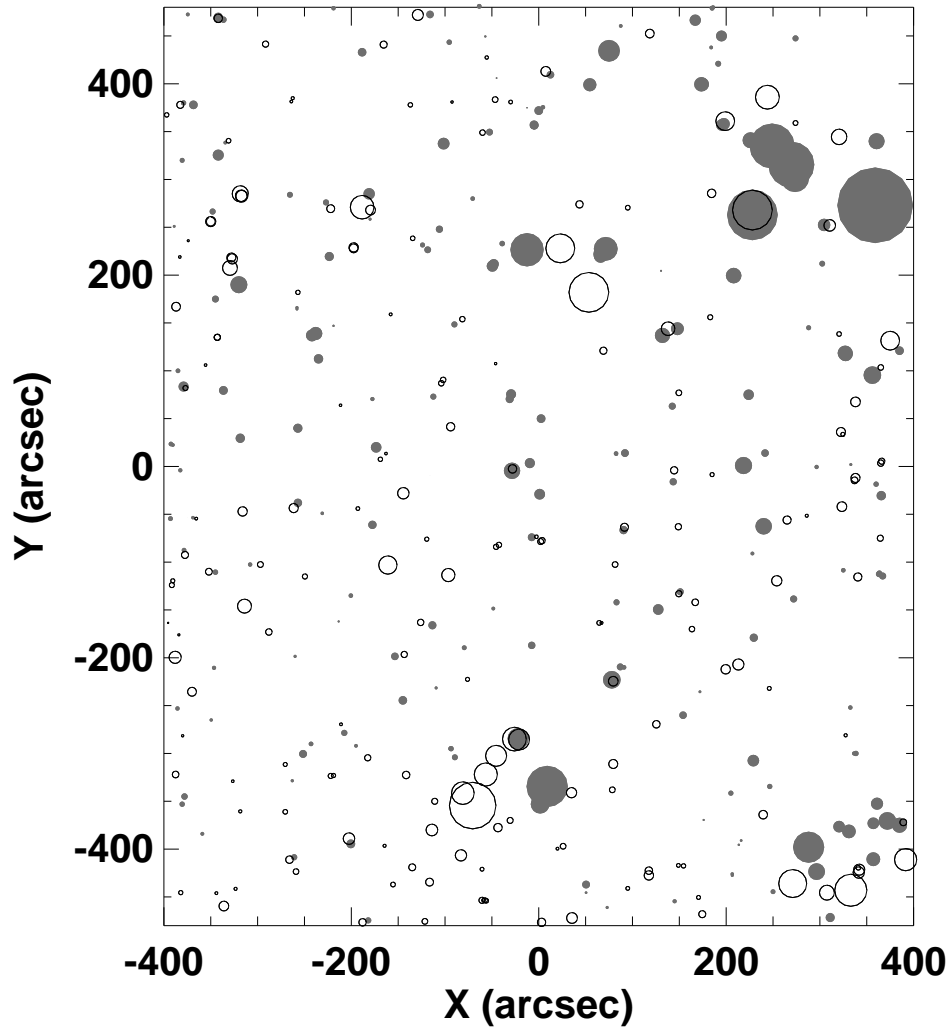


Fig. 5.— A plot showing the distribution of the RNFs (also see the accompanying movie3 for an example) in the solar disk in the FOV of 800×980 square arcsec on July 8, 2010. The size of circles represent that of the RNF flux, the largest size 5.85×10^{19} Mx, and the smallest 1.24×10^{17} Mx. Open circles indicate that the RNFs rotate clockwise, and filled circles, counter-clockwise.